EXPERIMENT OF STATIC AND DYNAMIC CHARACTERISTICS OF SPIRAL GROOVED SEALS

T. Iwatsubo, B.C. Sheng, and M. Ono
The Faculty of Engineering
Kobe University
Kobe, Japan

The leakages and the dynamic characteristics of six types of spiral grooved seals are experimentally investigated. The effect of the helix angle of the seal is investigated mainly under the conditions of the same nominal clearances, land and groove lengths, and groove depths. The dynamic characteristics are measured for various parameters such as preswirl velocity, pressure difference between inlet and outlet of the seal, whirling amplitude, whirling speed, and rotating speed of the rotor. The results are also compared with those of parallel grooved seals obtained previously. The results show that the leakage increases with the increase of the helix angle, but as the rotating speed increases, the leakages of the larger helix angle seals quickly drop. The leakage of the SS/SGR seal (smooth-stator/spiral-grooved-rotor seal) drops faster than that of the SGS/SR seal (spiral-grooved stator/smooth-rotor seal). It is found that a circumferential flow can be produced by the flow along the helix angle direction, and this circumferential flow acts as a negative swirl. For the present helix angle range, there is an optimum helix angle with which the seal has a comparatively positive effect on the rotor stability. Compared with the SGS/SR seals, the SS/SGR seal has a worse effect on the rotor stability.

1. INTRODUCTION

Spiral grooved seals used in turbopumps have the advantage of less leakage due to their pumping effect, and have a smaller possible contact area with the rotor in comparison to smooth seals. However, knowledge about their dynamic characteristics is very limited. In a theoretical study, Iwatsubo et al. (ref. 1) modeled the flows in the spiral grooved seals by considering the pumping effect due to the spiral grooves, and analyzed the static and dynamic characteristics of SS/SGR seals by a short-seal solution. In an experimental study, Kanki et al. (ref. 2) measured the static and dynamic characteristics of two SGS/SR seals with different lengths. Recently, Childs et al. (ref. 3) experimentally investigated six SGS/SR seals with different helix angles (15° ~ 70°). In practice, the small helix angle seals are usually used in conventional pumps. So the investigation of the small helix angle seals is necessary and important. Sometimes, the SS/SGR seals are also adopted in pumps due to their excellent pumping effect. But unfortunately, their dynamic characteristics have not been experimentally investigated yet.

In this experiment, the static and dynamic characteristics of the five SGS/SR seals and one SS/SGR seal are measured under the condition of asynchronous whirling motion. These seals have comparatively small helix angles (0.83° ~ 15.1°). The effects of the preswirl velocity, pressure difference between inlet and outlet of the seal, whirling amplitude, whirling speed, and rotor rotating speed on the static and dynamic characteristics of the seals are investigated. The results are also compared with those of the parallel grooved seal.

2. NOMENCLATURE

B	: Groove depths
C	: Radial clearance of seal
C_{xx}, C_{xy}	: Damping coefficients
e	: Whirling amplitude of rotor
F_x, F_y, F_r, F_θ	: Seal forces for x,y,r, and θ directions
K_{xx}, K_{xy}	: Stiffness coefficients
L	: Seal length
L_ℓ, L_g	: Land and groove widths
M_{xx}	: Inertia coefficients
N	: Number of lands or grooves
ΔP	: Pressure difference between inlet and outlet of seal
R, D	: Rotor radius and diameter
r, θ	: Radial and tangential coordinates
t	: Time
V_t	: Preswirl velocity
V_{ts}	: Preswirl velocity at zero rotating speed
x, y	: Fixed coordinates
α	: Helix angle
Ω	: Whirling speed of rotor
ω	: Rotating speed of rotor

3. TEST APPARATUS AND MEASUREMENT

The test apparatus has been illustrated in reference 4 in detail. So the apparatus is only outlined here. The assembly and layout of the test facility are shown in Fig. 1 and Fig. 2, respectively. The working fluid, that is water, is injected into the apparatus through three pairs of preswirl passages to yield different swirl velocities as shown in the cross section B of Fig. 1. The water passes through the clearance between the seal and rotor, then it flows through the outlets.

The preswirl velocity is adjusted by the six valves in order to obtain arbitrary values.

The bearing part which consists of two ball bearings is used to yield the rotating and whirling motions of the rotor. An inside sleeve and an outside sleeve which have 0.05 mm eccentricity to each other are attached between the two bearings, as shown in the cross section A. By rotating the two eccentric sleeves relatively, an arbitrary whirling amplitude can be adjusted in the range of 0 mm ~ 0.1 mm. The sleeves of both sides are synchronously driven by a motor through timing belts to obtain a whirling motion. The whirling speeds and their directions are controlled by an electric inverter. The rotating

speed and the direction of the rotor can also be changed by the other motor controlled by an electric inverter.

The geometries of the spiral grooved seals are shown in Fig. 3. There are five spiral-grooved-stator/smooth-rotor seals and one smooth-stator/spiral-grooved-rotor seal to be tested as shown in Table 1. These seals have the same nominal clearances, land and groove lengths, and groove depths, but they have different helix angles.

The measuring system consists of the measurements of rotating and whirling speeds of the rotor, pressure, preswirl velocity, leakage, fluid force, and displacement of the rotor. The fluid forces acting on the stator are measured by load cells as shown in the cross section C. The signals from the measuring instrument are recorded by a data recorder and analyzed by a computer.

The experimental conditions are shown in Table 2.

4. FLUID FORCE MODEL OF SEAL

For a small centered whirling motion of the rotor, the fluid reaction force in the seal can be represented as a linear function of the displacement, velocity and acceleration of the rotor, as follows:

$$-\begin{Bmatrix} F_x \\ F_y \end{Bmatrix} = \begin{bmatrix} M_{xx} & 0 \\ 0 & M_{xx} \end{bmatrix} \begin{Bmatrix} \ddot{x} \\ \ddot{y} \end{Bmatrix} + \begin{bmatrix} C_{xx} & C_{xy} \\ -C_{xy} & C_{xx} \end{bmatrix} \begin{Bmatrix} \dot{x} \\ \dot{y} \end{Bmatrix} + \begin{bmatrix} K_{xx} & K_{xy} \\ -K_{xy} & K_{xx} \end{bmatrix} \begin{Bmatrix} x \\ y \end{Bmatrix} \tag{1}$$

In the test, the whirling motion the rotor is given by

$$x = e \cos \Omega t, \qquad y - e \sin \Omega t \tag{2}$$

Substituting Eq. (2) into Eq. (1) and transferring the fixed coordinate system to a radial and tangential coordinate system, the following expressions are obtained.

$$\begin{aligned} -F_r/e &= -\Omega^2 M_{xx} + \Omega C_{xy} + K_{xx} \\ -F_\theta/e &= \Omega C_{xx} - K_{xy} \end{aligned} \tag{3}$$

To determine the dynamic coefficients of M_{xx},C_{xx},C_{xy},K_{xx} and K_{xy}, for a given rotating speed, F_r/e and F_θ/e are measured for the different forward and backward whirling speeds, then F_r/e is approximated by a quadratic function, and F_θ/e by a linear function of Ω. According to Eq. (3), inertia coefficient M_{xx}, damping coefficients C_{xx},C_{xy}, and stiffness coefficients K_{xx},K_{xy} are represented by the curvature, the slopes and the intercepts (at $\Omega = 0$) of the curves of F_r/e and F_θ/e, respectively.

5. TEST RESULTS AND DISCUSSION

5.1 Leakage

The seal leakages versus the pressure difference are shown in Fig. 4. As the helix increases, the leakages show a tendency to increase. The leakages

versus the rotating speed are shown in Fig. 5. The leakages of spiral seals drop monotonically with the increase of the rotating speed. It can be seen that the larger the helix angle is, the faster the leakage drops. The leakage of the SS/SGR seal (seal 7) is larger than that of the SGS/SR seal (seal 3), but with the increase of the rotating speed it quickly drops. Namely, the SS/SGR seal has the stronger pumping effect.

5.2 Fluid Force Coefficients
(a) Effect of rotating speed

The fluid force coefficients F_r/e and F_θ/e of parallel grooved seal 1, spiral grooved seal 3, and seals 5 and 7 are illustrated in Fig. 6. These results show that the radial force coefficients of seal 1, seal 3 and seal 7 almost do not vary with the rotating speed, but the radial force coefficient of seal 5 decreases with the increase of the rotating speed. In these seals, the tangential force coefficients tend to increase as the rotating speed increases. The tangential force coefficient of seal 7 increases at the fastest rate, and its sign varies from negative to positive, which means it has a negative effect on the rotor stability.

(b) Effect of preswirl velocity

Figure 7 shows the effect of preswirl velocities on the force coefficients of a parallel grooved seal (seal 1). From this figure, the effect of preswirl velocities on F_r/e can not be recognized, but the effect of preswirl velocities on F_θ/e is very distinct. The positive preswirl velocity causes F_θ/e to vary towards positive values, so that the unstable area is enlarged. The effect of the negative preswirl velocity on F_θ/e is exactly the opposite that of the positive preswirl velocity. The effect of preswirl velocities on the force coefficients of the spiral grooved seals is similar to that of the parallel grooved seal. To compare the effect of preswirl velocities on these seals, the upper limits of the unstable area, that is the intersections between the approximated lines of F_θ/e and axis of Ω/ω, are shown in Fig. 8. They are measured for different positive preswirl velocities. According to these results, as the helix angle α increases from 0° to 3.32°, the values of the upper limits decrease, but as the helix angle increases more than 3.32°, these values begin to increase. Seal 3 (α = 3.32°) has the minimum value which means the best effect on the rotor stability.

(c) Effect of pressure difference

The force coefficients are also measured for several pressure differences between the inlet and outlet of the seal. The results show that for different seals, the force coefficients only change their values, they do not change their qualitative characteristics. This tendency is similar to that of the parallel grooved seal. One of these results is shown in Fig. 9.

(d) Effect of whirling amplitude

Figure 10 shows the effect of whirling amplitude on the fluid force F_r and F_θ of seal 4. The results show that the absolute values of the fluid forces linearly increase with the increase of whirling amplitude. This means that under the present experimental conditions the relation between the fluid forces and the displacement can be correctly expressed by the approximated Eq. (1).

(e) Effect of helix angle

To compare the effects of the helix angles, the force coefficients of five seals measured under the same conditions are shown in Fig. 11. These force coefficients show the same qualitative tendencies. However, they show some quantitative differences. Though the preswirl velocity is not given ($V_{ts} = 0$), the tangential force coefficients of the spiral grooved seals show a result similar to that of the parallel grooved seal under a negative preswirl velocity (refer to Fig. 7). Namely, the unstable areas shift to the negative side of Ω/ω. Furthermore, the sequence of these values is the same as that of Fig. 8 in which seal 3 also has the minimum value. This phenomenon may be explained by the opposite circumferential flow caused by the helix angle. It is obvious that the fluid in the seal clearance will flow along the grooves, and the velocity of the flow can be divided into the circumferential and axial components. The circumferential velocity is just opposite to the rotating velocity of the rotor, because in order to obtain the pumping effect the rotor always rotates in the direction opposite to the helix direction. This circumferential flow, in fact, acts as a negative swirl. Both the parallel grooved seal and the vertical grooved seal ($\alpha = 90°$) do not produce this circumferential flow; therefore, at least one optimum helix angle with which the seal gets the maximum negative swirl ought to exist for a constant operating condition. For the present experimental condition, seal 3 ($\alpha = 3.32°$) is the optimum seal.

According to this discussion, a positive swirl also ought to be produced by the SS/SGR seal. Indeed, this phenomenon can be confirmed by the results shown in Fig. 12. This figure shows the force coefficients of the SGS/SR seal 3 and the SS/SGR seal 7. The results of the tangential force coefficients show that the SS/SGR seal is worse than the SGS/SR seal from the point of view of the rotor stability.

5.3 Stiffness, Damping, and Inertia Coefficients

The stiffness coefficients, damping coefficients and inertia coefficients of seal 1 - 5 are shown in Fig. 13. The inertia coefficients M_{xx} of the seals have the same tendencies, and they almost do not vary as the rotating speed. The direct damping coefficients C_{xx} are always positive and much larger than the cross-coupled damping coefficients C_{xy}. The parallel grooved seal has a relatively large C_{xx}, and the spiral grooved seal 5 has a relatively small C_{xx}. The cross-coupled damping coefficients C_{xy} are almost negative, which implies that there is a negative effect on the rotor stability according to Eq. (3). Seal 3 has a relatively small value of C_{xy}. The direct stiffness coefficients K_{xx} show the positive values, while the cross-coupled stiffness coefficients K_{xy} show values that are almost negative. So in general, these stiffness coefficients contribute to the stability of the rotor system. With the increase of the rotating speed, the direct stiffness coefficients K_{xx} of the larger helix angle seals tend to increase. Attention should be paid to the variation of K_{xy}. As the helix angle α increases from 0° to 3.32°, the values of K_{xy} decrease, but as the helix angle continues to increase, these values begin to increase. Seal 3 ($\alpha = 3.32°$) has the minimum value.

Childs et al. (ref. 3) investigated the static and dynamic characteristics of six SGS/SR seals with the comparatively large helix angles ($\alpha = 15° \sim 70°$). It should be pointed out that their dynamic coefficients are different from those of the present experiment. In the first place, their dynamic coefficients are obtained from a fixed axial Reynolds number over a range of rotating

speeds; while the present ones are obtained from a fixed rotating speed (equivalent to a fixed circumferential Reynolds number) over a range of rotating ratios (Ω/ω). Next, their dynamic coefficients are measured under the condition of synchronous rotor motion; while the present ones are measured under the condition of asynchronous rotor motion. For these reasons, the two results can not be compared directly. However, the two results have a similar effect on the stiffness coefficients for the helix angles. According to the results of Childs et al., the direct stiffness coefficient K_{ef} (equivalent to $-K_{xx}$, here) decreases at first, then increases as the helix angle α increases from 15° to 70°. The seal with the 30° helix angle has the minimum value of K_{ef}, which means it has a comparatively positive effect on the rotor stability.

The stiffness coefficients, damping coefficients and inertia coefficients of SGS/SR seal 3 and SS/SGR seal 7 are shown in Fig. 14. Seal 7 has relatively large values of C_{xx} and C_{xy}, which means the better damping effects in comparison with seal 3. For K_{xx} and K_{xy}, seal 7 also has the larger values. The increase of K_{xx} gives a positive effect to the rotor stability, but the increase of K_{xy} gives a negative effect to the rotor stability. In particular, when the rotating speed increases, K_{xy} of seal 7 tends to increase rapidly. According to K_{xy}, the SS/SGR seal is worse than the SGS/SR seal in rotor stability.

6. CONCLUSIONS

The static and dynamic characteristics of spiral grooved seals have been investigated and compared with those of a parallel grooved seal. The results of the spiral grooved seals and the parallel grooved seal show similar characteristics for the pressure difference and the whirling amplitude; however, the spiral grooved seals also show some specific characteristics, as follows:

(1) With the increase of the helix angle, the leakage increases, but as the rotating speed increases, the leakages of the larger helix angle seals quickly drop. The SS/SGR seal has a stronger pumping effect than that of the SGS/SR seal.

(2) For the SGS/SR seals, a circumferential flow can be produced by the flow along the helix angle direction, and this circumferential flow acts as a negative swirl. For this experimental helix angle range, an optimum helix angle exists with which the seal produces the maximum negative swirl. On the contrary, the SS/SGR seal produces a positive swirl velocity.

(3) The SS/SGR seal is worse than the SGS/SR seal in rotor stability.

REFERENCES

(1) Iwatsubo, T., Yang, B.C., and Ibaraki, R., "Theoretical Approach to Obtaining Dynamic Characteristics of Noncontacting Spiral-Grooved Seals," NASA CP-2443, 1986, pp. 155-187.

(2) Kanki, H., and Kwakami, T., "Experimental Study on the Static and Dynamic Characteristics of Screw Grooved Seals," ASME Design Tech. Conf. Pub. DE-Vol. 2, 1987, pp. 263-272.

(3) Childs, D.W., Nolan, S.A., and Kilgore, J.J., "Test Results for Turbulent Annular Seals, Using Smooth Rotors and Helically Grooved Stators," ASME Journal of Tribology (89-Trib-11) 1989.

(4) Iwatsubo, T., Sheng, B.C., and Matsumoto, T., "An Experimental Study on the Static and Dynamic Characteristics of Pump Annular Seals," NASA CP-3026, 1988, pp. 229-252.

Table 1 Seal dimensions

Seal	N	$\alpha(°)$	D(mm)	L/D	C(mm)	L_l(mm)	L_g(mm)	B(mm)
1 (GS/SR)	-	0	70.35	0.5	0.175	1.6	1.6	1.2
2 (SGS/SR)	1	0.83	70.35	0.5	0.175	1.6	1.6	1.2
3 (SGS/SR)	4	3.32	70.35	0.5	0.175	1.6	1.6	1.2
4 (SGS/SR)	8	6.65	70.35	0.5	0.175	1.6	1.6	1.2
5 (SGS/SR)	12	10.0	70.35	0.5	0.175	1.6	1.6	1.2
6 (SGS/SR)	18	15.1	70.35	0.5	0.175	1.6	1.6	1.2
7 (SS/SGR)	4	3.32	70.35	0.5	0.175	1.6	1.6	1.2

where GS/SR means grooved-stator / smooth-rotor.
SGS/SR means spiral-grooved-stator / smooth-rotor.
SS/SGR means smooth-stator / spiral-grooved-rotor.

Table 2 Experimental conditions

Pressure difference	ΔP(kPa)	294, 588, 784, 882
Rotating speed	ω (rpm)	$500 \sim 4500$
Whirling speed	Ω (rpm)	$\pm 600 \sim \pm 2400$
Whirling amplitude	e (μm)	$20 \sim 60$
Preswirl velocity	$V_t/\omega R$	$-2.59 \sim 2.75$
Temperature of water	T(°C)	19

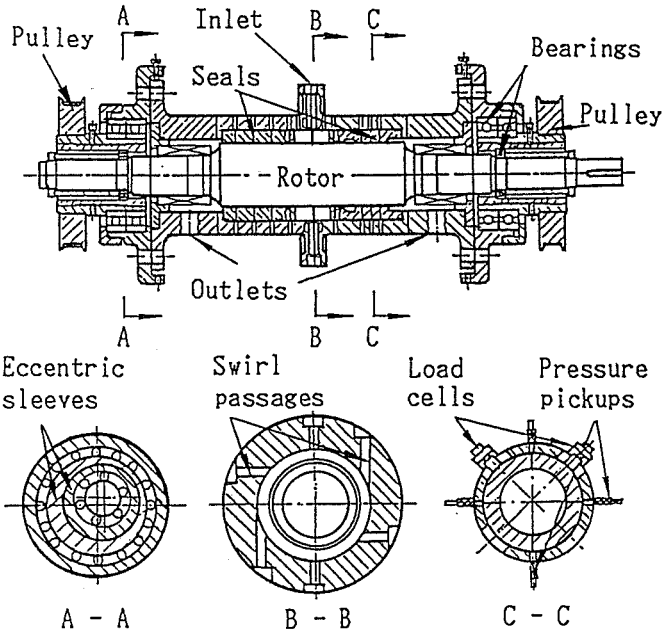

Fig. 1 Test apparatus assembly

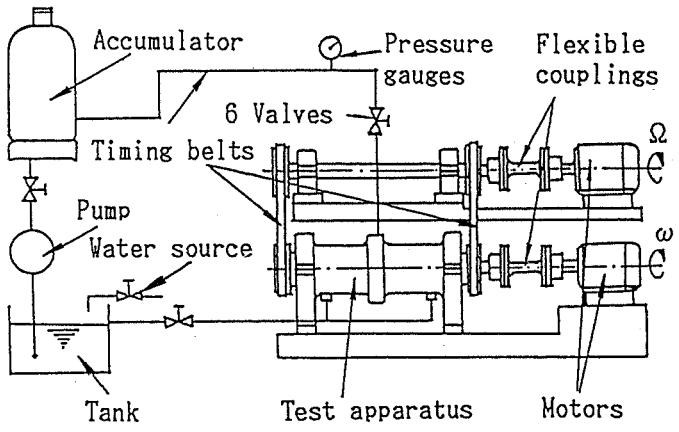

Fig. 2 Test facility layout

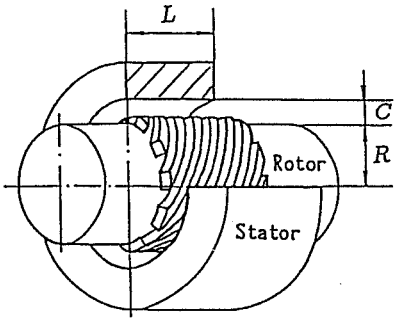

(a) Smooth-stator/spiral-grooved-rotor seal (SS/SGR seal)

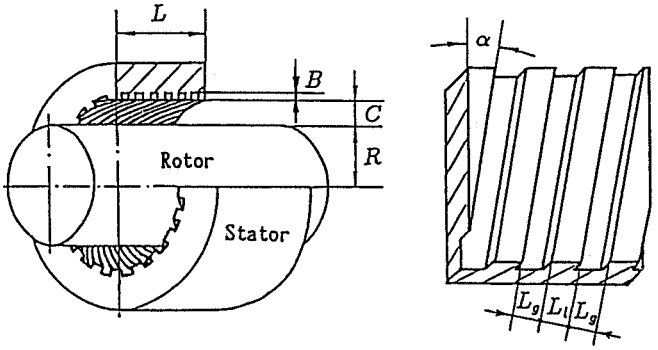

(b) Spiral grooved-stator/smooth-rotor seal (SGS/SR seal)

Fig. 3 Spiral grooved seals

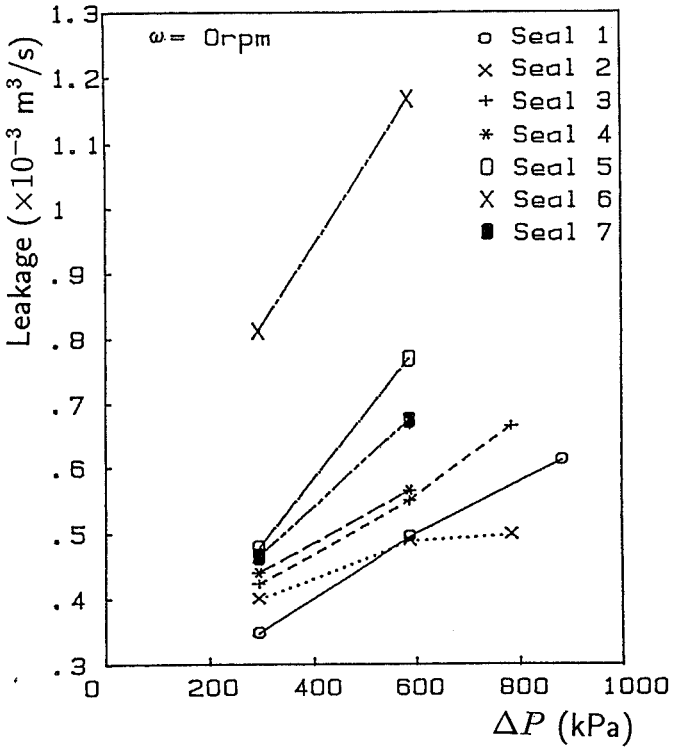

Fig. 4 Leakage versus ΔP

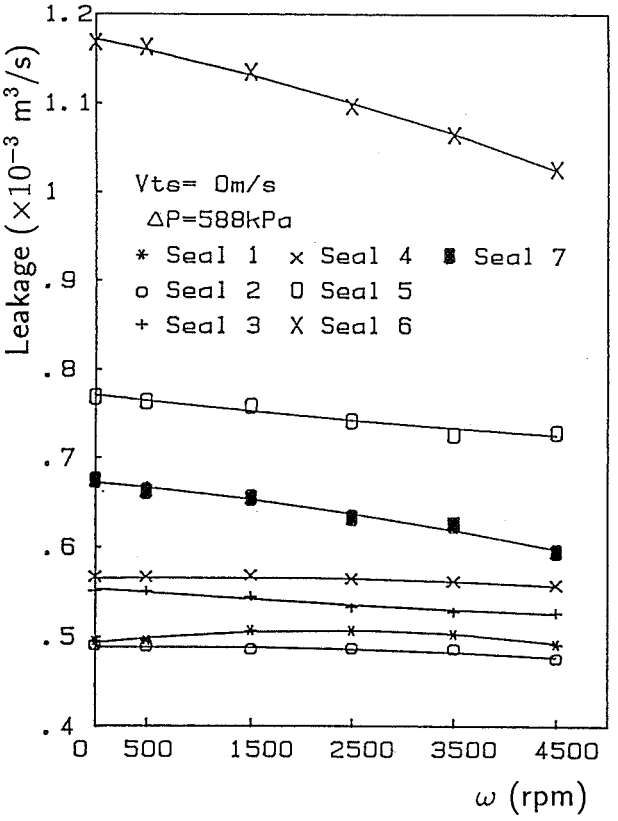

Fig. 5 Leakage versus rotating speed

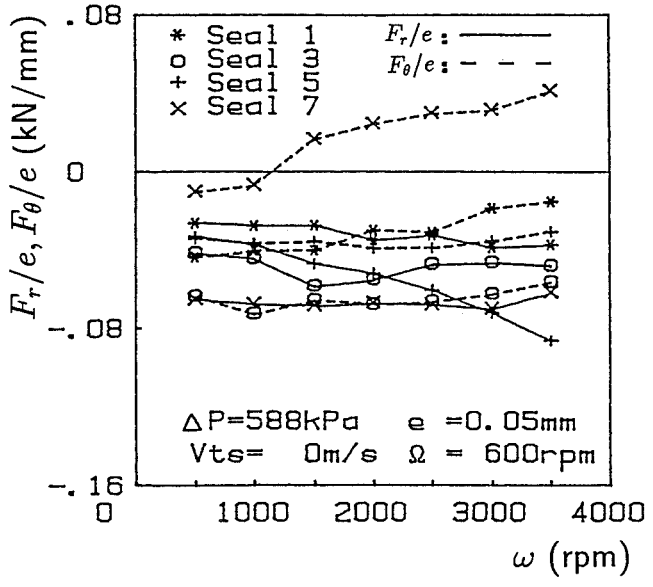

Fig. 6 Effect of rotating speed on F_r/e and F_θ/e

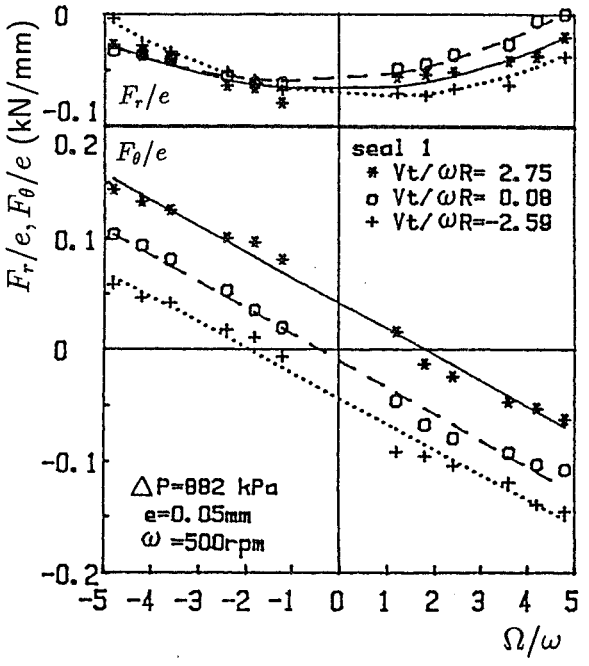

Fig. 7 Effect of preswirl velocity on F_r/e and F_θ/e for parallel grooved seal

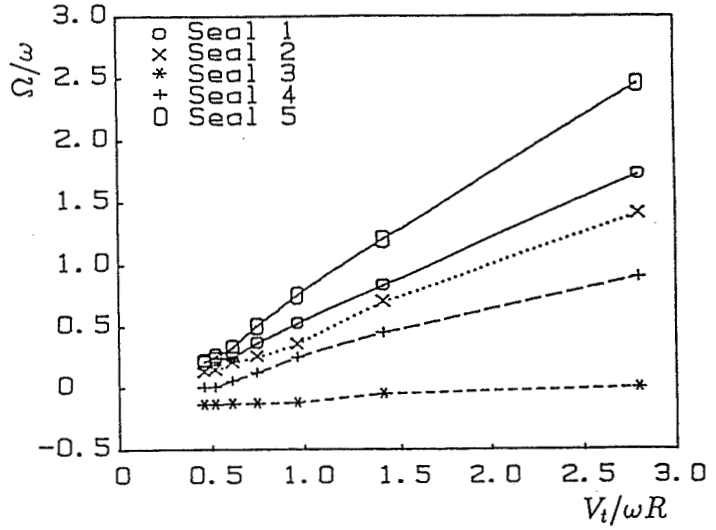

Fig. 8 Upper limit of unstable area for positive preswirl velocity

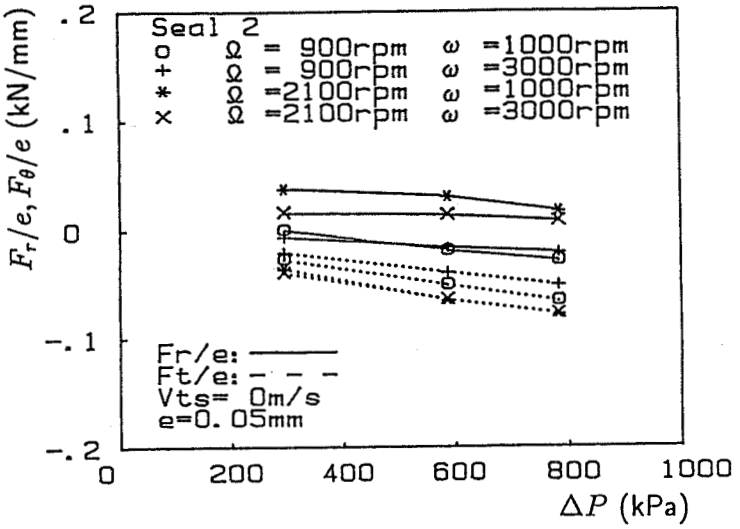

Fig. 9 Effect of pressure difference on F_r/e and F_θ/e

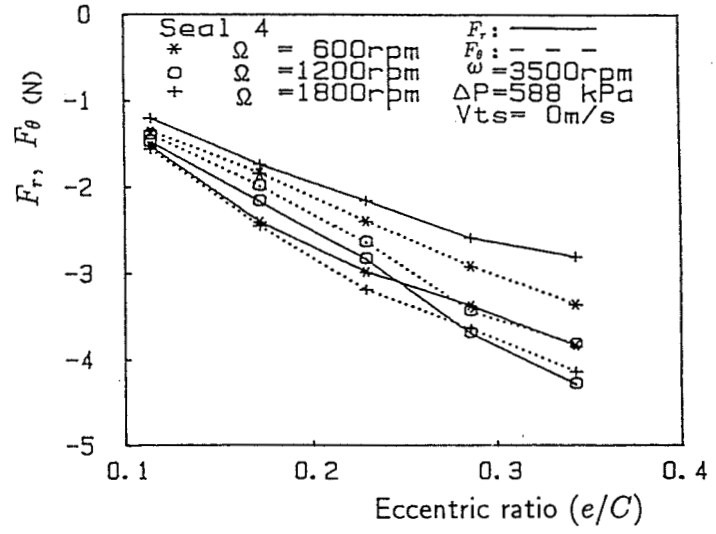

Fig. 10 F_r and F_θ versus eccentric ratio

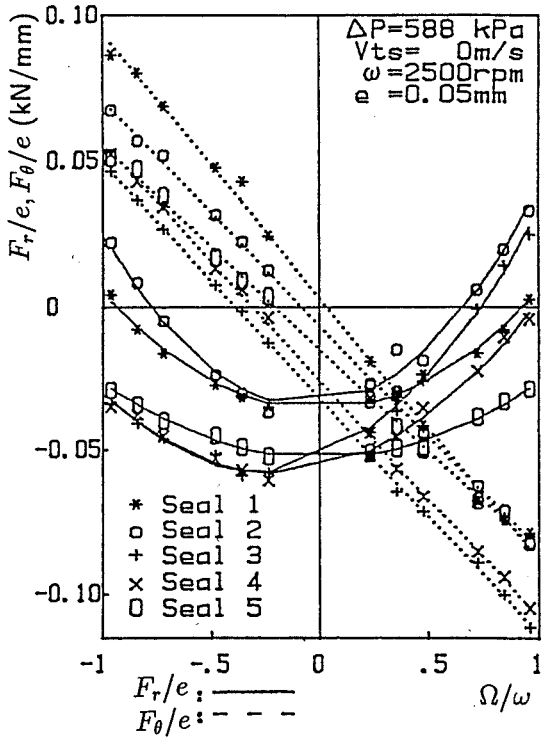

Fig. 11 Effect of helix angle on F_r/e and F_θ/e

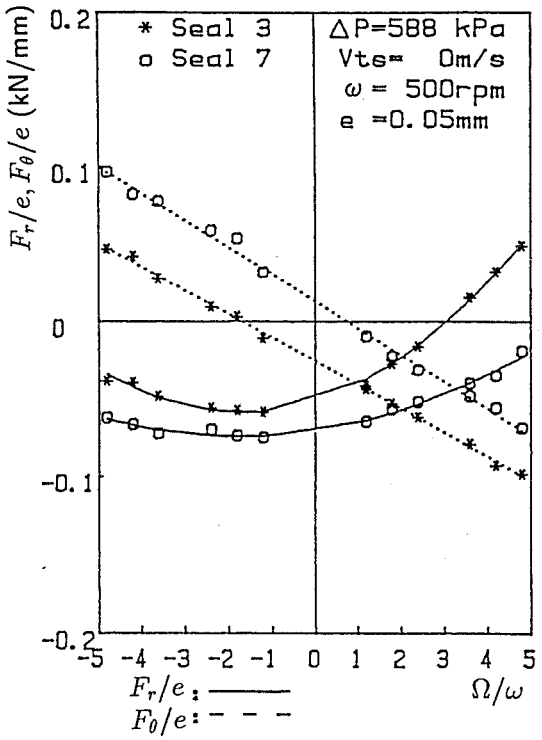

Fig. 12 Comparison of force coefficients for seal 3 and seal 7

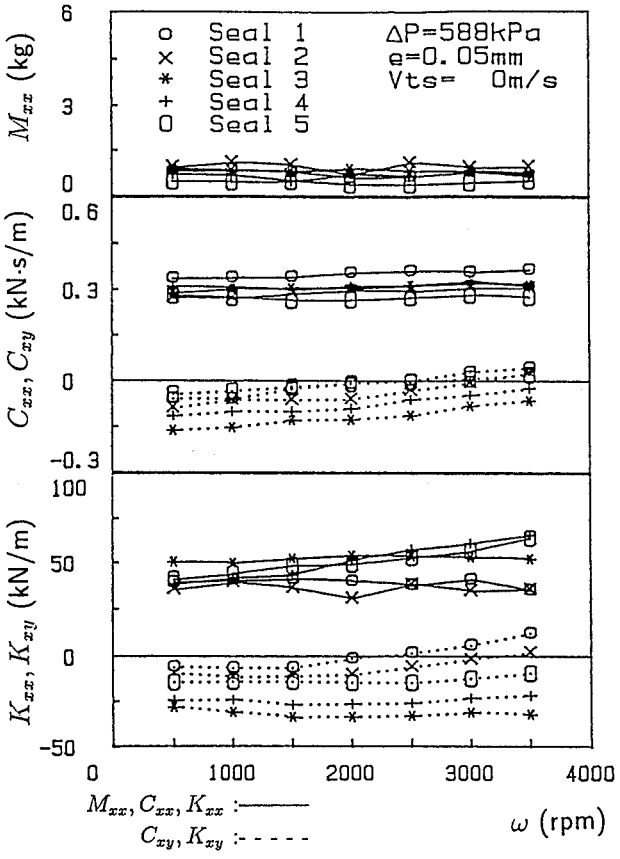

Fig. 13 Dynamic coefficients for rotating speed

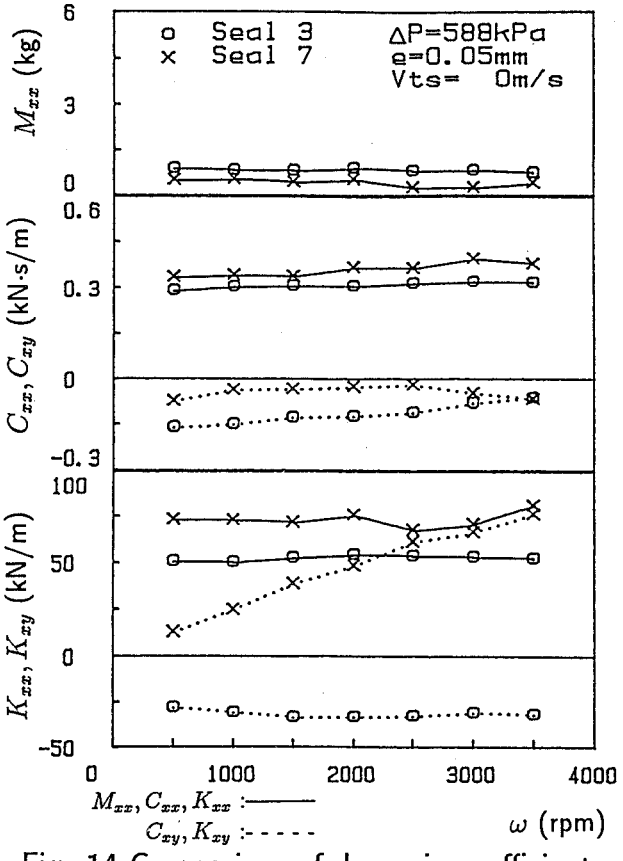

Fig. 14 Comparison of dynamic coefficients of seal 3 and seal 7